




# Explore Alteration of Lung and Gut Microbiota in a Murine Model of OVA-Induced Asthma Treated by CpG Oligodeoxynucleotides

Qingqing Wang , Jingjing Ji , Shuaijun Xiao , Jiong Wang, Xuebo Yan, Lei Fang

Department of Geriatric Respiratory and Critical Care, The First Affiliated Hospital of Anhui Medical University, Anhui Geriatric Institute, Hefei, Anhui, People's Republic of China

Correspondence: Jiong Wang, Email wangjiong7286@163.com

**Aim:** We sought to investigate the impact of CpG oligodeoxynucleotides (CpG-ODN) administration on the lung and gut microbiota in asthmatic mice, specifically focusing on changes in composition, diversity, and abundance, and to elucidate the microbial mechanisms underlying the therapeutic effects of CpG-ODN and identify potential beneficial bacteria indicative of its efficacy.

**Methods:** HE staining were used to analyze inflammation in lung, colon and small intestine tissues. High-throughput sequencing technology targeting 16S rRNA was employed to analyze the composition, diversity, and correlation of microbiome in the lung, colon and small intestine of control, model and CpG-ODN administration groups.

**Results:** (1) Histopathologically, both lung and intestinal tissue in asthmatic mice exhibited significant structural damage and inflammatory response, whereas the structure of both lung and intestinal tissue approached normal levels, accompanied by a notable improvement in the inflammatory response after CpG-ODN treatment. (2) In the specific microbiota composition analysis, bacterial dysbiosis observed in the asthmatic mice, accompanied by enrichment of Proteobacteria found to cause lung and intestinal epithelial damage and inflammatory reaction. After CpG-ODN administration, bacterial dysbiosis was improved, and a notable enrichment of beneficial bacteria, indicating a novel microecology. Meanwhile Oscillospira and Clostridium were identified as two biomarkers of the CpG-ODN treatment. (3) Heatmap analysis revealed significant correlations among lung, small intestine, and colon microbiota.

**Conclusion:** CpG-ODN treatment can ameliorate OVA-induced asthma in mice. One side, preserving the structural integrity of the lung and intestine, safeguarding the mucosal physical barrier, the other side, improving the dysbiosis of lung and gut microbiota in asthmatic mice. Beneficial bacteria and metabolites take up microecological advantages, regulate immune cells and participate in the mucosal immune response to protect the immune barrier. Meanwhile, Oscillospira and Clostridium as biomarkers for CpG-ODN treatment, has reference significance for exploring precise Fecal microbiota transplantation treatment for asthma.

**Keywords:** microbiota, lung-gut axis, CpG Oligodeoxynucleotides, 16S ribosomal RNA, asthma

## Introduction

Asthma is a heterogeneous chronic respiratory disease affects more than 300 million people globally and more than 30 million people in China, with a death rate of 49.2 per 100,000, which creates a serious economic burden on the society and families.<sup>1,2</sup> Many phenotypes of adult asthma have been described, but the mechanisms for most remain incompletely understood. Asthma characterized by predominant type 2 inflammation is the best understood endophenotype, exhibit an imbalance in Th1/Th2 cells and a predominant Th2 immune response. The conventional treatment for asthma is based on glucocorticoids, primarily aimed at alleviating clinical symptoms without altering the disease's progression and prognosis. However, due to a lack of responsiveness to classical glucocorticoid inhalation therapy among many patients, traditional treatment options are increasingly being questioned. Therefore, it becomes crucial to explore non-steroidal alternatives for asthma management.

Based on the hygiene hypothesis proposed over 30 years ago, numerous studies have substantiated that sufficient exposure of humans to bacterial components such as endotoxin and DNA through PRRs can activate innate immunity in the host, thereby diminishing the risk of atopy and asthma in children.<sup>3,4</sup> Subsequent research has demonstrated that the immunostimulatory effect

of DNA relies on its unmethylated CpG motifs.<sup>5,6</sup> Toll-like receptors (one kind of PRRs) have been extensively investigated for their potential application in asthma treatment.<sup>7</sup> The synthetic unmethylated oligonucleotide CpG-ODN exhibits structural similarity to bacterial DNA and elicits immune responses akin to natural CpG motifs, rendering it extensively employed in the treatment of asthma, cancer, and other atopic disorders.<sup>8–10</sup> Numerous animal and clinical studies have demonstrated that CpG-ODN induces the production of a wide range of cytokines and chemokines, including IFN- $\alpha$ , TNF- $\alpha$ , and IL-12, through its interaction with TLR9 on PDCs as well as T cell and B cell endosomes. These potent modulators effectively promote Th1-type immune responses, thereby establishing a Th1-dominant immunological milieu. Augmenting the Th1 immune response or activating regulatory T cells represents a promising strategy to significantly alleviate asthma by counterbalancing the prevailing Th2 immune response, which can directly ameliorate the atopic responses of asthma, including mitigating airway inflammation and bronchial hyperreactivity.<sup>10–12</sup>

Notably, in the study conducted by Takuma Okajima et al, CpG-ODN was observed to attenuate Th2 responses in the lungs of asthmatic mice, nevertheless, no activation of Th1 or regulatory responses was detected in the bronchoalveolar lavage fluid, lung transcripts, or serum of asthmatic mice treated with CpG-ODN.<sup>13</sup> This suggests that CpG-ODN may be implicated in alternative mechanisms for the treatment of asthma. Epidemiological studies have demonstrated that environmental exposures related to asthma can better account for the significant increase in asthma prevalence observed over the past few decades. Many of these exposures are associated with early-life events that shift the microbiota, including prenatal and perinatal antibiotic use, cesarean section delivery, urban living conditions, and formula feeding practices.<sup>7,14–18</sup> With the advancement of microbiome and metabolomics research, the role of microbiome and its metabolites in asthma's pathogenesis and progression has gained increasing attention from researchers. Numerous studies have shown that changes in lung and gut microbes, as well as their metabolic profiles during early life, can directly affect the host's immune response and alter susceptibility to asthma. The latest research has demonstrated that CpG-ODN can rapidly induces a(1,2)-fucosylation in the epithelial cells of the mouse small intestine (IEC). This process plays a pivotal role in maintaining diverse and robust microbiota homeostasis, facilitating symbiotic interactions between hosts and microbiota, as well as preventing excessive colonization by opportunistic pathogens.<sup>19–21</sup> Further research suggested that the oral administration of ODNcap can elicit intestinal mucosal immunity.<sup>13,22,23</sup> Based on these studies have prompted us to consider the potential involvement of lung and gut microbes as well as their metabolites in the treatment of asthma with CpG-ODN. Therefore we established an OVA-induced asthma model and explored the histological changes, composition, diversity, and abundance of microbiota in the lungs and intestines before and after treatment of CpG-ODN, and to elucidate the microbial mechanisms underlying the therapeutic effects of CpG-ODN in asthma treatment and identify potential beneficial symbiotic bacteria indicative of its efficacy.

## Materials and Methods

### Reagents and Instruments

Ovalbumin OVA, chloral hydrate, 4% paraformaldehyde fixative, saline, PBS, and aluminum hydroxide mixture were purchased from Solebo Biotechnology Co., LTD. CpG-ODN 1668 (5'-TCC ATG ACG TTC CTG ATG CT-3'): Produced by Shanghai Shenggong Biological Engineering Co., Ltd.

### Experimental Animals

A total of 24 female SPF BALB/c mice aged 7 weeks were routinely raised in SPF Barrier Animal Experimental center. Animal experiments were carried out in accordance with the code of Practice of the Animal Research Ethics Committee of Anhui Medical University (license number: LLSC20221231). Feed: provided by Jiangsu Synergy Pharmaceutical and Biological Engineering Co., LTD., in compliance with the implementation standard GB14924.3–2010 “Nutritional composition of Laboratory Animal Compound Feed”.

### OVA-Induced Asthma Model and CpG-ODN Treatments

Twenty-four mice were randomly allocated into three groups: a normal control group, an OVA model group, and a CpG-ODN administration group, with eight mice in each group. In the OVA model group, after seven days of adaptive feeding, the animals received intraperitoneal injections of a mixture containing 20 $\mu$ g OVA and 1mg aluminum hydroxide on days 0, 7,

and 14 of the experiment. On days 21 and 22, the mice were challenged with a 1% OVA suspension through aerosol inhalation for thirty minutes. In the CpG-ODN administration groups (which underwent the same sensitization process as the OVA model group), abdominal injections of CpG-ODN - including one hundred grams (CpG-ODN 1668 (5'-TCC ATG ACG TTC CTG ATG CT-3')) were administered three hours before atomization inhalation on days twenty-one and twenty-two.<sup>24,25</sup> The dose of CpG-ODN administered to mice in CpG-ODN administration groups was maintained consistently throughout the duration of the study. The control group treated with PBS at corresponding experimental time points.

## Histopathological Staining of the Lung and Gut Tissue

After twenty-four hours from their last administration, all mice were sacrificed; part of their lung tissue along with small intestine tissue and colon tissue were fixed in 4% paraformaldehyde for over 24 hours, followed by paraffin sectioning. The organizational structure changes were observed under an optical microscope (NIKON ECLIPSE E100) using HE staining, and photographs were taken. The inflammatory scores of lung tissue were assessed based on parameters such as alveolar wall thickening, epithelial cell alterations, and infiltration of inflammatory cells. Similarly, the inflammatory scores of the small intestine were determined by evaluating changes in villus structure, epithelial morphology, and presence of infiltrating inflammatory cells. Additionally, the scoring system for colon inflammation included assessment of crypt alterations, loss of goblet cells, and infiltration of inflammatory cells.

## 16S rRNA Gene Sequence Data Processing

The V3-V4 regions of 16S rRNA gene were amplified with the forward primer (5'-ACT CCT ACG GGA GGC AGC A-3') and reverse primer (5'-GGA CTA CHV GGG TWT CTA AT-3') in QIIME 2(2019.4). Amplicon sequence variants (ASVs) as well as operational taxonomic units (OTUs) were determined using DADA2 and Vsearch, and matched to taxonomies using the Green genes and SILVA database. Alpha diversity for each sample was calculated, including Chao 1, Observed species, Shannon and Simpson indices (number and relative distribution of taxa) and Beta diversity, which additionally weights phylogenetic relationships. Bray-Curtis measures, were calculated to evaluate between-sample compositional differences by means of ordination analyses and in PERMANOVA tests with clinical and inflammatory variables. Linear discriminant analysis effect size (LEfSe), performed in Python LEfSe package, were used to identify species differ clearly in different groups (normal group vs model group vs CpG-ODN administration group).

## Statistical Analysis

The paired end Illumina MiSeq sequences were analysed using the QIIME2 (2019.4) software, PICRUST2 software, R software package (R version 3.6), and Python LEfSe package. SPSS software (version 27.0; IBM, Armonk, NY, USA) was used for the remaining data analysis tasks. Analysis of variance was utilized to test parameters while the Kruskal-Wallis test was applied for nonparametric testing purposes. To account for multiple testing, p-values were corrected using the Bonferroni method. P values of less than 0.05 were considered statistically significant. The permutation test was employed for significance analysis and quantification of the degree of difference through ADONIS, a nonparametric multivariate analysis of variance. Here, Pr represents the P value, where  $P < 0.05$  is considered statistically significant. The R2 value signifies the interpretation of sample differences based on various grouping factors, with a higher R2 indicating greater dissimilarity between groups.

## Results

### Histological Alterations of Lung Tissue and Intestinal Tract

Hematoxylin and Eosin (HE) staining results indicated that in the control group, a higher number of alveoli presented with a clear structure and thin walls (indicated by the blue arrow), with no detectable inflammatory cell infiltration within the tissue. In the model group, the number of alveoli declined, with some alveoli experiencing atrophy and collapse. Epithelial cell hyperplasia gave rise to thickening of the alveolar walls (as indicated by the red arrow), accompanied by a considerable infiltration of inflammatory cells into the tissue (as indicated by the black arrow). In contradistinction to the model group, the severity of lung injury in the treatment group was conspicuously alleviated, and the counts of atrophied and collapsed alveoli as well as inflammatory cells were significantly diminished (Figure 1A). In the control group, a larger number of villi were present in

the mucous layer of the small intestine, which were neatly and closely arranged. Epithelial cells did not undergo degeneration or shedding (as indicated by the black arrow), and goblet cells were more plentiful (as indicated by the red arrow). In the model group, intestinal impairment was manifest, the mucous layer thinned, the number of villi decreased significantly, the remaining villi were shorter (as indicated by the black arrow), and the number of goblet cells decreased significantly (as indicated by the red arrow). Simultaneously, lymph node enlargement (as indicated by the yellow arrow) was noted. The degree of intestinal injury in the treatment group was significantly ameliorated in comparison with that in the model group, and the numbers of villi and goblet cells in the mucous layer increased (Figure 1B). In the control group, the crypts within the mucous layer of the colon were closely arrayed, featuring abundant goblet cells and intact epithelium, with no discernible inflammatory cell infiltration. In the model group, the intestinal structure was disordered, presenting ulcers in some areas, epithelial cell erosion and shedding, and the lamina propria exposed (green arrow), while the crypts vanished and a considerable number of fibrous tissues and inflammatory cell proliferation were observable (yellow arrow). The intestinal damage in the treatment group was significantly ameliorated compared with that in the model group, with a small number of epithelial cells eroded and shed (green arrow), no reduction in crypts, and an increase in goblet cells (Figure 1C).

## Alteration of Structure and Diversity of Lung and Gut Microbiota

In lung, colon and small intestine, the number of ASVs in the normal group, model group and CpG-ODN administration group was 3768, among which the number of ASVs only in the normal group was 26426, ASVs only in the model group was 24975, ASVs only in the drug administration group was 25969 (Figure 2A). Compared with normal group, the

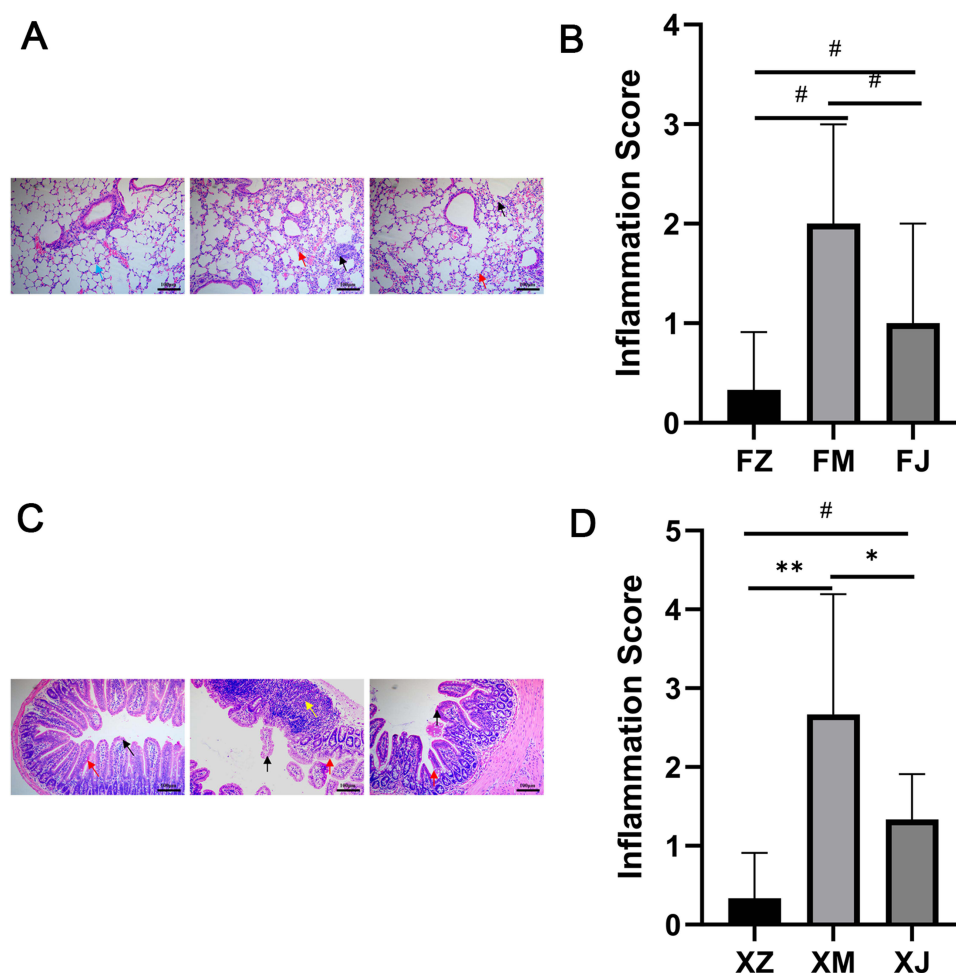
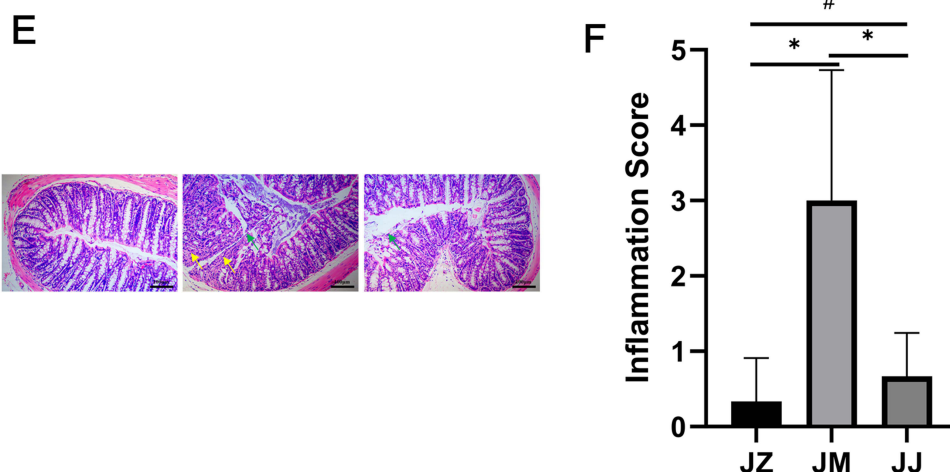
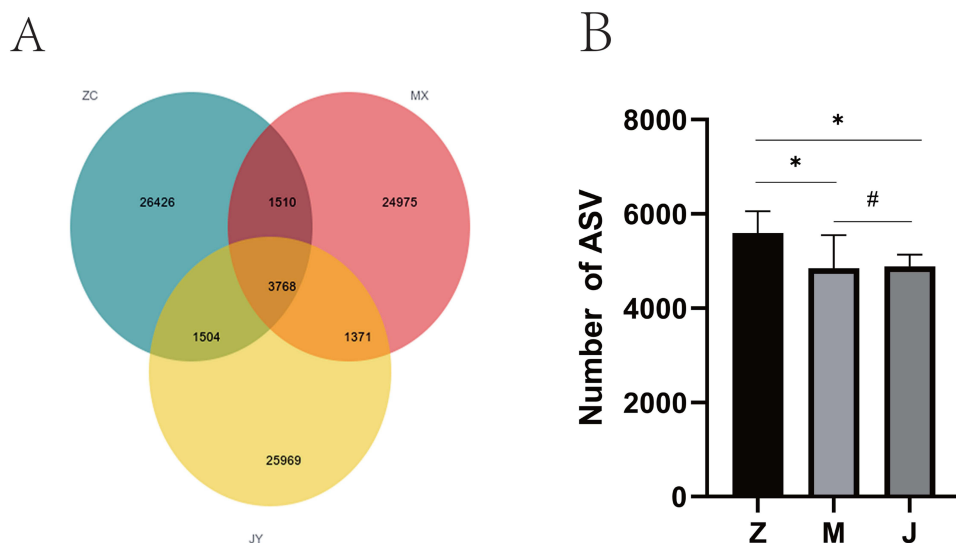


Figure 1 Continued.



**Figure 1** (A) The histopathological changes in the lungs. The CpG-ODN group exhibited a significant improvement in the degree of lung injury compared to the model group, with a notable reduction in the number of atrophic and collapsed alveoli as well as inflammatory cells. From left to right, the images represent the normal group, model group, and CpG-ODN group, respectively. In the lung control group, the alveolar wall at the blue arrow was thin, in the model group, alveolar wall at the red arrow was thickened, a large number of inflammatory cells were infiltrated at the black arrow, in the CpG-ODN group, alveolar wall at the red arrow was thin, and a small number of inflammatory cells were infiltrated at the black arrow; (B) Statistical significance analysis of lung inflammation scores. There was no statistically significant difference in the level of pulmonary inflammatory response among the three groups. FZ, FM, and FJ represent the normal, model, and CpG-ODN administration group of the lungs, respectively. ( $\#P > 0.05$ ); (C) The histopathological changes in the small intestine. From left to right, the images represent the control group, model group, and CpG-ODN group, respectively. In the control group, the epithelial cells were intact at the black arrow, and a large number of goblet cells at the red arrow, in the model group, villi were shortened at the black arrow, goblet cells decreased at the red arrow, and lymph node enlargement occurred at the yellow arrow. In the CpG-ODN administration group, goblet cells were abundant in the red arrow and villi were intact in the black arrow. (D) Statistical significance analysis of small intestine inflammation scores. There was a statistically significant difference in the level of intestinal inflammatory response among the three groups. The intestinal inflammatory response in the model group exhibited a significantly higher level compared to that in the normal group, whereas the CpG-ODN administration group demonstrated a significant improvement in the inflammatory response when compared to the model group. XZ, XM, and XJ represent the normal, model, and CpG-ODN administration group of the small intestine, respectively ( $\#P > 0.05$ ,  $*P < 0.05$ ,  $**P < 0.01$ ). (E) The histopathological changes in the colon. From left to right, the images represent the control group, model group, and CpG-ODN group, respectively. In the control group, the crypts of the colon mucosa were densely arranged, exhibiting a rich presence of goblet cells. The epithelium remained intact without any noticeable infiltration of inflammatory cells. In the model group, a large number of fibrous tissue and inflammatory cells proliferated at the yellow arrow, the lamina propria was exposed and the crypt disappeared at the green arrow, in the CpG-ODN administration group, a small amount of epithelial cells were eroded and shed at the green arrow. (F) Statistical significance analysis of colon inflammation scores. There was a statistically significant difference in the level of intestinal inflammatory response among the three groups. The intestinal inflammatory response in the model group exhibited a significantly higher level compared to that in the normal group, whereas the CpG-ODN administration group demonstrated a significant improvement in the inflammatory response when compared to the model group. JZ, JM, and JJ represent the normal, model, and CpG-ODN administration group of the colon. ( $\#P > 0.05$ ,  $*P < 0.05$ ).



**Figure 2** (A) ASV number of mice in different groups: the normal(ZC), model(MX) and CpG-ODN administration group(JJ), ASV sequence number of the set of unique and Shared; (B) Statistical analysis of the number of ASVs in the normal group, the model group, and CpG-ODN administration group: Compared with normal group, the number of ASV in model group and CpG-ODN administration group were significantly decreased ( $\#P > 0.05$ ,  $*P < 0.05$ ), suggested the microbial diversity was significantly reduced in model group and CpG-ODN group compared to the control group.



number of ASV in model group and CpG-ODN administration group were significantly decreased ( $P = 0.022$ ,  $P = 0.028$  Figure 2B), suggested the microbial diversity was significantly reduced in model group and CpG-ODN administration group compared to the control group.

In Alpha diversity analysis, the Chao1 and Observed species indices serve as indicators of microbial richness in the sample and provide estimates of the actual number of species present in the community. Meanwhile, the Shannon and Simpson indices reflect microbial diversity. The results demonstrated that the Chao1 and Observed species indices in the lung, colon, and small intestine of both the model group and CpG-ODN administration group were significantly lower compared to those of the normal group, particularly in the lung ( $P=0.015$ ,  $P=0.0068$  Figure 3A). The Shannon and Simpson indexes of the model group and the CpG-ODN administration group in the small intestine were observed to be lower compared to the normal group ( $P=0.014$ ,  $P=0.014$  Figure 3B). The Shannon index and Simpson index in the colon were higher in both the model group and the CpG-ODN administration group compared to the normal group; however, these differences did not reach statistical significance (Figure 3C). These findings suggest a decrease in microbial abundance and diversity in the lung and small intestine of model group and CpG-ODN administration group. Notably, while there was a decrease in the total number of microorganisms in the colon but an increase in diversity. This observation highlights a significant disparity in population Alpha diversity between asthmatic mice and normal mice. In Beta diversity analysis, PCoA analysis were used to compare community structure similarity, closer distances indicated higher levels of community similarity across different samples. To statistically evaluate the results of the PCoA analysis, we employed ADONIS analysis, which not only assesses the significance of differences but also quantifies the magnitude of dissimilarity between groups using R2 values. The findings revealed significant disparities in microbial composition among the lung, colon, and small intestine; however, the dissimilarities observed between the lung and gut were more pronounced compared to those between the colon and small intestine. This suggests a greater divergence in microbial composition between the lung and gut while indicating a higher degree of similarity in microbial communities between the colon and small intestine. (Figure 3D, Table 1)

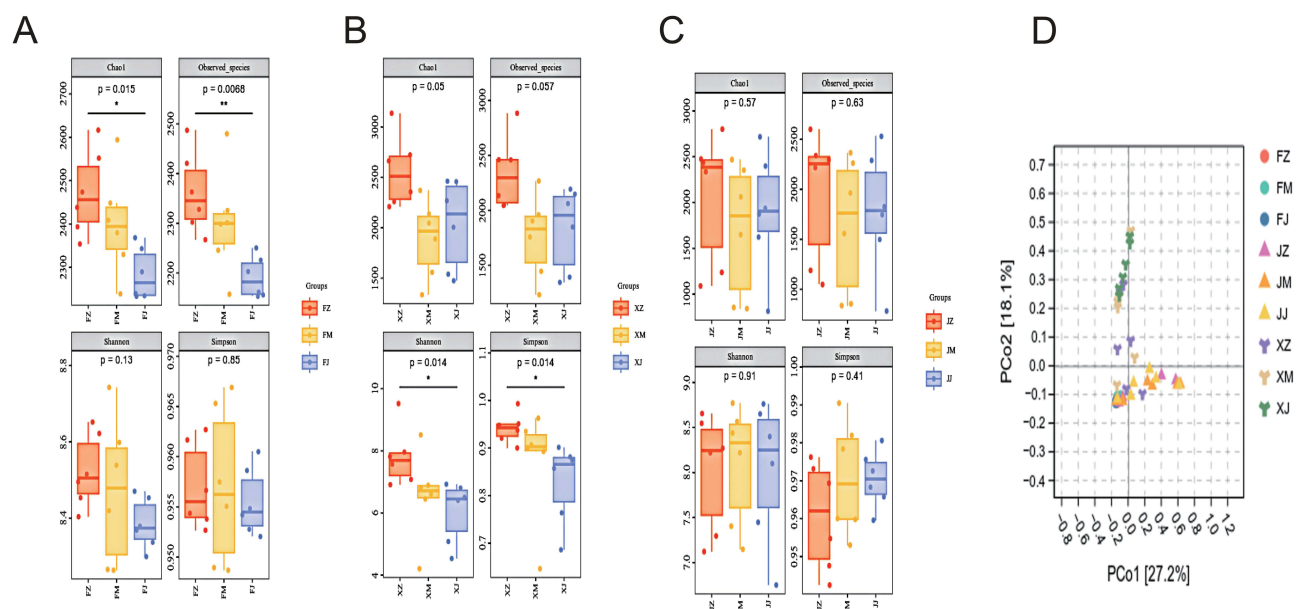


**Figure 3** The lung and intestinal microbiota of the model and CpG-ODN group mice are disrupted, with changes in richness and diversity. (A–C) Alpha diversity analysis: Chao1, Observed species, Shannon, and Simpson indices are used to compare the microbial richness and diversity between the three groups of lung, small intestine and colon. (D): PCoA analysis: The similarity between the lung, colon, and small intestine was reflected based on the distance matrix. The projection distance indicates the degree of sample difference, with smaller distances indicating greater similarity. The smaller the projection distance, the smaller the sample differences. (In the figure, FZ FM FJ represents the normal lung group, model group, and CpG-ODN group, JZ JM JJ represents the normal colon group, model group, and CpG-ODN group, and XZ XM XJ represents the normal small intestine group, model group, and CpG-ODN group).

**Table 1** ADONIS analysis: To Assess the Significance of Differences as Well as Quantify the Magnitude of Dissimilarity Between Lung and Gut Groups Using R2 Values

Group	Df	SumOfSqs	R2	F	Pr(>F)
F vs X	1	0.239295012343872	0.55190390823121	41.8765823325758	0.001
F vs J	1	0.209042730525048	0.351306091525182	18.4130095192961	0.001
X vs J	1	0.130633617078227	0.288159698126152	13.7635221137359	0.001

**Note:** Grouping: F means lung groups; X means small intestine groups; J means colon groups. As can be seen from the figure, the pairwise comparisons of lung, colon and small intestine all showed  $P < 0.05$ , indicating that the microbial composition of the three sites was significantly different. The R2: lung and small intestine was 0.55190390823121, R2: lung and colon was 0.351306091525182, R2: small intestine and colon was 0.288159698126152, indicating that there is a greater dissimilarity in the microbial composition between the lung and gut, while the microbial communities of the colon and small intestine exhibit more similarity.

## Specific Community Composition of Lung and Gut Microbiota

Specific lung and intestinal bacterial taxa were detected in the normal, model and CpG-ODN administration group. In the normal lung, colon, and small intestine groups exhibited a detection of 41, 38, and 41 bacterial phyla, 236, 247 and 243 genera respectively; while the model group showed a detection of 39, 38, and 42 phyla, 237, 221 and 223 genera respectively; Similarly, in the CpG-ODN administration group, there were detections of 40, 41, and 36 phyla, 228, 246 and 226 genera respectively (Figures 4 and Table 2). By analyzing the relative abundance of the top 20 phyla and genera in terms of species composition, we compared the variations in bacterial abundance in the lung, small intestine and colon, among the normal group, model group, and CpG-ODN administration group (Figure 5A and B).

In the lung control group, Proteobacteria, Firmicutes, Bacteroidetes, Acidobacteria, Cyanobacteria, Actinobacteria, Fusobacterium, Chloroflexi and Gemmatimonads were identified as the predominant phyla. Lactobacillus, Rhodobacter, Thermomonas, Escherichia and Allobaculum were found to be the dominant genera. In the lung CpG-ODN administration group the abundance of Chloroflexi was significantly lower compared to that in the normal group ( $P=0.008$  Table 3), while Nitrospirae abundance in the CpG-ODN administration group was significantly lower than that in the model group ( $P=0.015$  Table 3). In the colon control group, Proteobacteria, Firmicutes, Bacteroidetes, Actinobacteria, Cyanobacteria, Acidobacteria and Fusobacteria were identified as the predominant phyla, Lactobacillus, Rhodobacter,

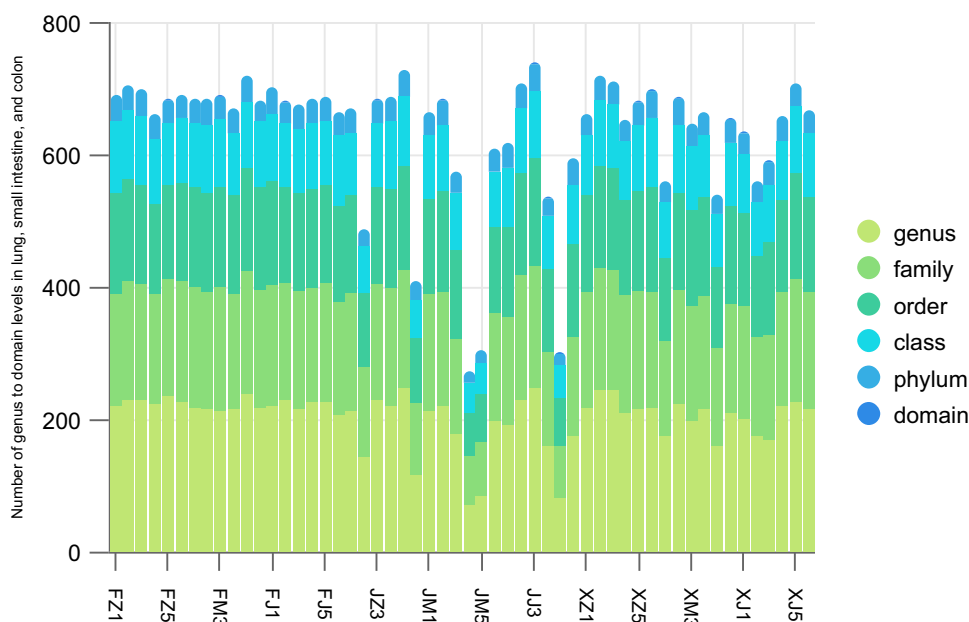


**Figure 4** The number of phylum to genus levels detected in the lung, colon and small intestine samples of the three groups of mice.

**Table 2** Number of Genus to Domain Levels Contained in Each Specimen of Lung, Small Intestine, and Colon

Number of Genus to Domain Levels Contained in Each Specimen of Lung, Small Intestine, and Colon						
ID	Domain	Phylum	Class	Order	Family	Genus
FZ1	I	41	107	152	170	219
FZ2	I	38	103	154	180	229
FZ3	I	39	104	151	176	228
FZ4	I	38	98	136	167	222
FZ5	I	35	93	143	175	236
FZ6	I	34	100	148	183	225
FM1	I	37	97	149	184	217
FM2	I	39	103	151	176	214
FM3	I	35	101	153	186	213
FM4	I	37	93	152	173	215
FM5	I	40	99	157	185	237
FM6	I	33	96	159	177	216
FJ1	I	40	101	157	184	219
FJ2	I	32	95	147	177	228
FJ3	I	36	98	148	178	215
FJ4	I	37	99	149	172	226
FJ5	I	37	96	147	181	226
FJ6	I	36	107	143	173	205
JZ1	I	38	94	147	178	213
JZ2	I	25	72	112	137	141
JZ3	I	35	96	148	174	229
JZ4	I	38	100	152	175	221
JZ5	I	39	106	156	179	247
JZ6	I	28	58	98	107	117
JM1	I	34	95	145	176	213
JM2	I	38	100	152	171	221
JM3	I	33	85	135	143	178
JM4	I	18	45	65	74	70
JM5	I	21	46	71	82	84
JM6	I	35	85	129	164	196
JJ1	I	37	89	137	161	192
JJ2	I	37	99	155	187	229

(Continued)



**Table 2** (Continued).

Number of Genus to Domain Levels Contained in Each Specimen of Lung, Small Intestine, and Colon						
ID	Domain	Phylum	Class	Order	Family	Genus
JJ3	I	41	103	160	187	246
JJ4	I	28	79	125	142	160
JJ5	I	18	50	73	78	81
JJ6	I	39	92	137	152	174
XZ1	I	31	92	147	174	217
XZ2	I	36	100	154	185	243
XZ3	I	33	96	153	184	243
XZ4	I	32	91	140	179	210
XZ5	I	35	98	152	179	215
XZ6	I	41	105	161	173	217
XM1	I	32	84	124	146	173
XM2	I	42	100	150	170	223
XM3	I	33	98	143	176	196
XM4	I	36	93	150	171	214
XM5	I	30	79	123	149	158
XM6	I	35	95	148	167	208
XJ1	I	33	90	139	171	200
XJ2	I	30	81	122	151	174
XJ3	I	34	89	139	160	167
XJ4	I	36	90	141	170	220
XJ5	I	35	102	158	186	226
XJ6	I	36	96	145	176	214

Thermomonas and Escherichia were found to be the predominant genera. In the colon model group, there was a significant increase in the abundance of Deferribacteres and Desulfovibrio compared to that in the normal group ( $P=0.033$  Table 4,  $P=0.033$  Table 5), while Candidatus Arthromitus showed a decrease ( $P=0.017$  Table 5). The CpG-ODN administration group exhibited higher abundance of tretinspirillum compared to the normal group ( $P=0.052$  Table 5). In the control group of the small intestine, Proteobacteria, Firmicutes, Bacteroidetes, Actinobacteria, Cyanobacteria, Acidobacteria, Fusobacteria and Chloroflexi were identified as the predominant phyla. The dominant genera included Candidatus Arthromitus, Lactobacillus, Rhodobacter, Thermomonas, Escherichia, Allobaculum, Desulfovibrio and Hydrogenophaga. Compared to the normal group, Gemmatimonadetes and Nitrospirae showed a decrease in abundance in the model group ( $P<0.01$ ,  $P=0.043$  Table 6). In the CpG-ODN administration group there was a decrease in abundance of Chloroflexi, Acidobacteria, Gemmatimonadetes and Nitrospirae, while an increase of Candidatus Arthromitus was observed ( $P=0.017$  Table 7).

Considering the potential oversight of certain bacterial taxa with lower abundance but significant functional impact, LEfSe analysis identify the most notable species in the lung, colon, and small intestine in different groups. (Figure 6A–F,

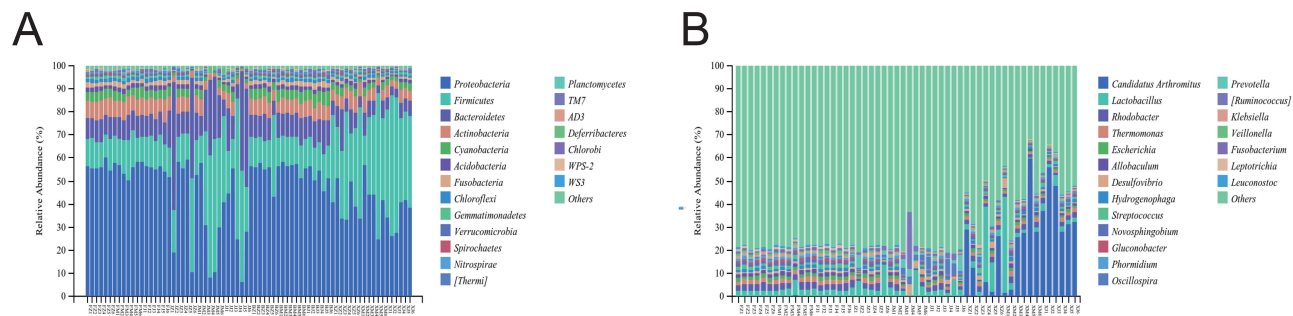


**Figure 5** Microecological characteristics of microflora at phyla and genus level in the control, model, CpG-ODN administration groups of lung, small intestine and colon. **(A)** shows the analysis of species composition at phylum level for each sample of lung, colon, and small intestine. **(B)** shows the analysis of species composition at genus level for each sample of lung, colon, and small intestine. (FZ, FM, and FJ represent the normal, model, and CpG-ODN administration group of the lungs; JZ, JM, JJ represent the normal, model, and CpG-ODN administration group of the colon; XZ, XM, XJ represent the normal, model, and CpG-ODN administration group of the small intestine).

LDA threshold of 2). In **Figure 6A**, three distinct clusters were observed in the lung model group, with *Candidatus Arthromitus* being predominant. Similarly, the CpG-ODN group also exhibited three clusters, with *atopobium* as the dominant species. In the colon model group, 10 clusters were identified, with the *Deferribacteres* phylum and its subphylum being predominant, whereas in the CpG-ODN group, 2 clusters were detected, with *Oscillospira* as the dominant genus. In the small intestine model group, three clusters were identified, with GN02 as the predominant phylum, *Erwinia* and *Variovorax* as the dominant genera, whereas in the CpG-ODN group, 8 clusters were detected, both *Clostridia* and *Candidatus Arthromitus* as the dominant genus. The relatedness of the identified bacterial species and significant distinctions across all levels are depicted in **Figure 6B–D**, and **F**.

In conclusion, bacterial dysbiosis could be observed in the asthmatic mice, most abundant phyla was *Proteobacteria* (such as *Erwinia* and *desulfovibrio* genus) were found to be enriched in the model group usually caused lung and intestinal epithelial damage and inflammatory reaction. However, after the CpG-ODN administration, the bacterial

**Table 3** Phyla with Statistically Significant Differences Between Control, Model, and CpG-ODN Administration Groups in Lung Microbiota

	FZ(N=6)	FM(N=6)	FJ(N=6)	F	P
Chloroflexi	0.0165676967±0.0012	0.015232875±0.0014	0.0140821783±0.0016 <sup>a</sup>	4.67	0.027
Nitrospirae	0.0045895567±0.0007	0.00497947±0.0007 <sup>b</sup>	0.0035992533±0.0011	4.002	0.04

**Notes:** <sup>a</sup>for statistical differences with FZ, <sup>b</sup>for statistical differences with FJ, using ANOVA test method. In the phylum of Chloroflexi F=4.67, P=0.027, so Chloroflexi in the three groups of lung are statistically different. Pairwise comparison between groups showed that FZ and FJ were significantly different (P<0.05), so there is a statistical difference between FZ and FJ (P<0.05). In the phylum of Nitrospirae F=4.002, P=0.04, so Nitrospirae in the three groups of lung are statistically different. Pairwise comparison between groups showed that FM and FJ were significantly different (P<0.05), so there is a statistical difference between FM and FJ (P<0.05).

**Table 4** Phyla with statistically significant differences between control, model, and CpG-ODN administration groups in colon microbiota

	JZ(N=6)	JM(N=6)	JJ(N=6)	F	P
Deferribacteres	0.0003746150 (0.000144635, 0.0005070750)	0.00395699 (0.0004975275, 0.0154921725) <sup>a</sup>	0.00190296 (0.00092448, 0.007397525) <sup>b</sup>	7.942	0.019

**Notes:** <sup>a,b</sup>for statistical differences with JZ, comparisons were corrected using the Bonferroni method. The median (P25, P75) of Deferribacteres abundance values in three groups were as follows: 0.0003746150 (0.0001446350, 0.0005070750), 0.0039569900 (0.0004975275, 0.0154921725), 0.0019029600 (0.0009244800, 0.0073975250), using Kruskal–Wallis test F=7.942, P=0.019, so Deferribacteres in the three groups of colon are statistically different. Pairwise comparison between groups showed that JZ and JM were significantly different (P<0.05), and there is a statistical difference between JZ and JJ (P<0.05).

**Table 5** Genus with Statistically Significant Differences Between Control, Model, and CpG-ODN Administration Groups in Colon Microbiota

	JZ(N=6)	JM(N=6)	JJ(N=6)	F	P
Candidatus Arthromitus	0.0007825 (0.000315045, 0.001143075)	0.000136335 (0.00, 0.000311943) <sup>a</sup>	0.000384560 (0.000309275, 0.000902705)	8.35	0.015
Desulfovibrio	0.00712504 (0.005688675, 0.00825412)	0.0180266 (0.008566, 0.03189134) <sup>b</sup>	0.008295255 (0.0058278875, 0.01719163)	6.678	0.035
Oscillospira	0.00321869 (0.001553835, 0.0066050875)	0.023564695 (0.0038114525, 0.029503675)	0.03139676 (0.0081130925, 0.058788695)	6.222	0.045

**Notes:** <sup>a,b</sup>for statistical differences with JZ, comparisons were corrected using the Bonferroni method. The median (P25, P75) of Candidatus Arthromitus abundance values in three groups were as follows: 0.000782500 (0.000315045, 0.001143075), 0.000136335 (0.000000000, 0.000311943), 0.000384560 (0.000309275, 0.000902705), using Kruskal–Wallis test F=8.35, P=0.015, so Candidatus Arthromitus in the three groups of colon are statistically different. Pairwise comparison between groups showed that JZ and JM were significantly different (P<0.05). The median (P25, P75) of Desulfovibrio abundance values in three groups were as follows: 0.00712504 (0.005688675, 0.00825412), 0.0180266 (0.008566, 0.03189134), 0.008295255 (0.0058278875, 0.01719163), using Kruskal–Wallis test F=6.678, P=0.035, so Desulfovibrio in the three groups of colon are statistically different. Pairwise comparison between groups showed that JZ and JM were significantly different (P<0.05). The median (P25, P75) of Oscillospira abundance values in three groups were as follows: 0.00321869 (0.001553835, 0.0066050875), 0.023564695 (0.0038114525, 0.029503675), 0.03139676 (0.0081130925, 0.058788695), using Kruskal–Wallis test F=6.222, P=0.045, so Oscillospira in the three groups of colon are statistically different. Pairwise comparison of results showed no significant difference after correction, but it is worth noting that the comparison between JJ and JZ before correction, P<0.05, showed a statistical difference.

**Table 6** Phyla with Statistically Significant Differences Between Control, Model, and CpG-ODN Administration Groups in Small Intestine Microbiota

	XZ(N=6)	XM(N=6)	XJ(N=6)	F	P
Chloroflexi	0.0111133567±0.0014	0.0102600283±0.0032	0.008586235±0.0013	9.29	0.032
Acidobacteria	0.018078265±0.0043	0.0125783317±0.0056	0.011384545±0.0033 <sup>a</sup>	3.746	0.048
Gemmatimonadetes	0.0091207350±0.0014	0.0057786083±0.0009 <sup>b</sup>	0.0056194183±0.0016 <sup>a</sup>	13.125	<0.001
Nitrospirae	0.00458815±0.0023	0.0027308383±0.0008 <sup>b</sup>	0.0025129917±0.0008 <sup>a</sup>	3.706	0.049

**Notes:** <sup>a,b</sup>for statistical differences with XZ, using ANOVA test method. Within the Chloroflexi phylum, the abundance does not exhibit homogeneity of variance, thus necessitating the use of the Welch test; whereas for other phyla where homogeneity of variance is met, the ANOVA test is employed. In the phylum of Chloroflexi F=9.29, P=0.032, so Chloroflexi in the three groups of Intestine are statistically different. No significant difference found in pairwise comparison. In the phylum of Acidobacteria F=3.746, P=0.048, so Acidobacteria in the three groups of Intestine are statistically different. Pairwise comparison between groups showed that XZ and XJ were significantly different (P<0.05), so there is a statistical difference between XZ and XJ (P<0.05). In the phylum of Gemmatimonadetes F=13.125, P<0.001, so Gemmatimonadetes in the three groups of Intestine are statistically different. Pairwise comparison between groups showed that XZ and XJ were significantly different (P<0.05), so there is a statistical difference between XZ and XJ (P<0.05), as well as XZ and XM (P<0.05), so there is a statistical difference between XZ and XM (P<0.05). In the phylum of Nitrospirae F=3.706, 0.049, so Nitrospirae in the three groups of Intestine are statistically different. Pairwise comparison between groups showed that XZ and XJ were significantly different (P<0.05), so there is a statistical difference between XZ and XJ (P<0.05), as well as XZ and XM (P<0.05), so there is a statistical difference between XZ and XM (P<0.05).

**Table 7** Genus with Statistically Significant Differences Between Control, Model, and CpG-ODN Administration Groups in Small Intestine Microbiota

	XZ(N=6)	XM(N=6)	XJ(N=6)	F	P
Candidatus Arthromitus	0.09357874 (0.0131702, 0.269075605)	0.264599935 (0.0258009625, 0.3588659725)	0.34629442 (0.3066240975, 0.4998878775) <sup>a</sup>	8.035	0.018

**Notes:** <sup>a</sup>for statistical differences with XZ, comparisons were corrected using the Bonferroni method. The median (P25, P75) of Candidatus Arthromitus abundance values in three groups were as follows: 0.09357874 (0.0131702, 0.269075605), 0.264599935 (0.0258009625, 0.3588659725), 0.34629442 (0.3066240975, 0.4998878775), using Kruskal–Wallis test F=8.035, P=0.018, so Candidatus Arthromitus in the three groups of Intestine are statistically different. Pairwise comparison between groups showed that XZ and XJ were significantly different (P<0.05), so there is a statistical difference between XZ and XJ (P<0.05).

dysbiosis was improved, and the beneficial commensal bacteria significantly enriched, meanwhile Oscillospira and Clostridium were identified as two biomarkers of the CpG-ODN treatment using Iefse analysis.

## Heatmap Analysis

To further explore the association between lung and gut microbiota, Pearson correlation coefficient was used to correlate the top 20 species with phylum and genus-level abundance values of lung and gut microbiota on the heatmap. Figure 7A and B show the species with the most significant correlations between lung and small intestine and lung and colon at the phylum level,

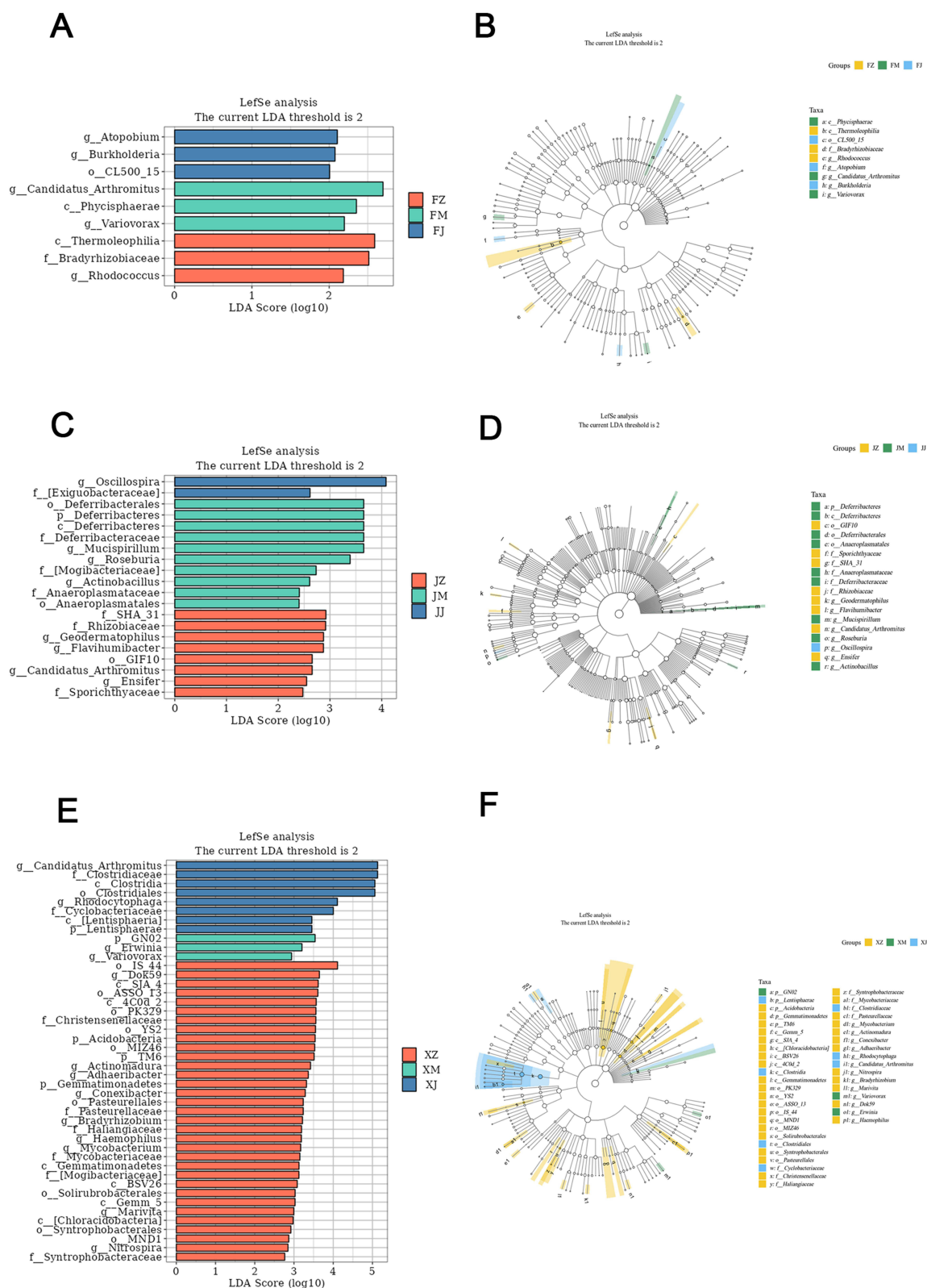
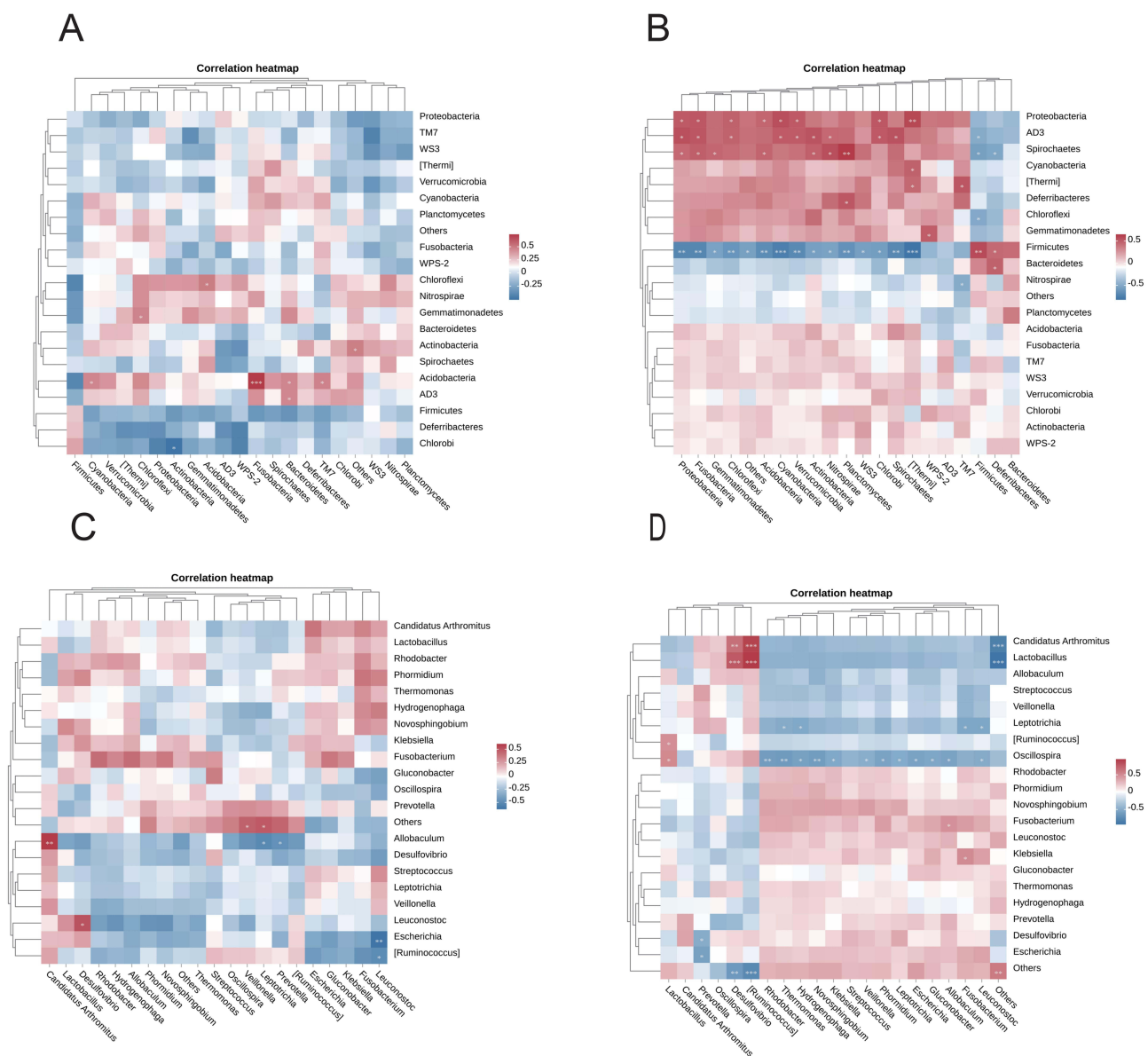


**Figure 6** Linear discriminant analysis was conducted on three distinct groups (**A**) (lung), 6C (colon), and 6E (intestine)). A histogram visualized this analysis's scores highlighting statistically significant differences among biomarkers across these groups. Species influence was depicted through varying bar lengths within this histogram representation. Additionally, a cladogram (**B–D**, and **F**) showcased hierarchical classification from phylum to species level using concentric circles where each smaller circle denoted a specific taxon and the diameter of the circle is proportional to the relative abundance. Core bacterial populations for each group were represented as yellow, blue, and green dots respectively.



respectively, and Figure 7C and D show the most significant correlations between lung and small intestine and lung and colon at the genus level, respectively.

The results demonstrated that, at the phylum level, Acidobacteria in the lung exhibited a positive correlation with four phyla in the small intestine, with Firmicutes being the most statistically significant ( $P < 0.001$ ). Chloroflexi in the lung showed a positive correlation with Acidobacteria in the small intestine ( $P < 0.05$ ), and Gemmatimonadetes displayed a positive correlation with Chloroflexi in the small intestine ( $P < 0.05$ ). Conversely, Chlorobi in the lung exhibited a negative correlation with Actinobacteria in the small intestine ( $P < 0.05$ ). Proteobacteria, Spirochaetes, and AD3 in the lung were positively correlated with multiple phyla of colon, respectively. On the other hand, Firmicutes in the lung displayed a negative correlation with multiple phyla of colon, particularly Cyanobacteria and Thermi ( $P < 0.001$ ). At genus level analysis revealed that Allobaculum in the lung was positively correlated with Candidatus Arthromitus found within small intestines ( $P < 0.01$ ), while



negatively correlated with *Prevotella* and *Leptotrichia* (both  $P < 0.01$ ). Both *Escherichia* and *Ruminococcus* within lungs were negatively correlated to *Leuconostoc* found within small intestines ( $P < 0.01$ ,  $P < 0.05$ ). *Candidatus Arthromitus* as well as *Lactobacillus* in the lung showed positive correlations to *Ruminococcus* and *Desulfovibrio* respectively ( $P < 0.001$  for both correlations), whereas *Ruminococcus* in the lung along *Oscillospira* presented positive correlations to *Lactobacillus* in colon ( $P < 0.05$ , for both correlations).

## Discussion

The involvement of the digestive system often accompanies many respiratory diseases, such as asthma. Similarly, patients with inflammatory bowel disease or irritable bowel syndrome may experience pulmonary involvement, which is characterized by inflammation or impaired lung function.<sup>26</sup> Studies have demonstrated that patients with asthma exhibit structural and functional alterations in the intestinal mucosa.<sup>27</sup> In this current investigation, we observed similar manifestations in asthmatic mice. Histological examination using HE staining revealed pronounced inflammation in the small intestine and colon of mice in the model group, characterized by epithelial goblet cell loss and mucosal crypt loss. Importantly, Jian Wang et al also reported significant intestinal injury in a respiratory influenza model, highlighting the requirement for gut microbiota involvement in such injury.<sup>14,15</sup> Commensal microbial colonization within both the gastrointestinal and respiratory tracts has evolved over an extended period to establish resistance against pathogens and promote pathogen clearance.<sup>16</sup> Disruption of these microbial communities often leads to various disease states known as dysbiosis, including metabolic and immune disorders,<sup>17</sup> which may constitute an important aspect of asthma pathogenesis.<sup>18</sup>

In the analysis of species diversity in this study, the number of ASVs serves as an indicator for overall microbial diversity. Both the OVA model group and CpG-ODN administration group showed a significant reduction in ASV numbers, indicating impaired microbial diversity in both lungs and gut during asthma. Specifically, Alpha diversity analysis revealed a decrease in both total microorganism count and diversity within lung and small intestine model groups as well as administration group. However, there was an increase in diversity specifically within the colon despite a decrease in total microorganism count. Species composition analysis demonstrated distinct compositions of lung and gut microbiota among normal, asthma, and CpG-ODN administration groups. Additionally, we noted that bacterial dysbiosis could be observed in the asthmatic mice, most abundant phyla was Proteobacteria (such as *Erwinia* and *desulfovibrio* genus) were found to be enriched in the model group usually caused lung and intestinal epithelial damage and inflammatory reaction.<sup>28–30</sup> However, the administration of CpG-ODN resulted in significant modifications to the microecology of the microbiota, leading to a remarkable enrichment of beneficial symbiotic bacteria. Through Iefse analysis, we identified significantly increased marker microorganisms such as *treponspirillum* and *Clostridium* within the CpG-ODN treatment group. Previous studies have demonstrated a negative association between *Spirillum tremulum* and asthmatic stridor, potentially attributed to its polyamine metabolites.<sup>31</sup> Additionally, *Oscillospira*, a member of the Firmicutes phylum, plays a crucial role in the production of butyric acid, a short-chain fatty acid (SCFA), which exerts protective effects on intestinal epithelial cells by modulating the expression of MUC2, an intestinal mucus protein. Moreover, It also contributes to maintaining the integrity of the intestinal epithelial barrier by modulating TWK-related potassium channel 1 (Trek-1).<sup>32–34</sup> *Clostridium* species stimulate the generation of ILCs that produce IL-22 and contribute to reinforcing the epithelial barrier function. Clusters IV, XIVa, and XVIII within the genus *Clostridium* induce expansion and differentiation of Treg cells by providing bacterial antigens and creating a TGF- $\beta$ -rich environment. This directly enhances their anti-inflammatory effect on gut health. Furthermore, induced Treg cells also promote IgA production in the gut while regulating mucosal immune responses and mediating protective effects against asthma.<sup>33,35–37</sup>

Studies have demonstrated that the lung and gut microbiota, along with their metabolites, exert an influence on host local mucosal immunity through the lung-gut axis, thereby significantly impacting the endocrine, metabolic, and immune systems.<sup>26,38,39</sup> The mucosal barrier serves as a physical defense mechanism comprising biochemical and immunological components that act as the primary line of defense against pathogen invasion. To safeguard the host during respiratory tract diseases, administration of microorganisms (eg, probiotics), substances promoting their growth (eg, prebiotics), or microbial metabolites (eg, SCFA) can be employed to facilitate direct competition with pathogenic microorganisms and enhance epithelial physical and immune barrier function.<sup>40–44</sup> Studies have demonstrated that the integrity of the mucosal barrier is compromised in sepsis and acute respiratory distress syndrome, leading to bacterial translocation from the gastrointestinal



tract to the lungs. In cases of acute lung injury, there is a transient transfer of bacteria into the bloodstream, resulting in a significant increase in cecal bacterial load. Furthermore, short-chain fatty acids (SCFA), which are metabolites produced by gut microbiota, can enter circulation and influence bone marrow hematopoiesis while impairing dendritic cells' ability to induce TH2 cell-mediated allergic respiratory inflammation.<sup>45</sup> In future investigations, fluorescence imaging technology holds promise for tracking microbiota within the human body and further elucidating their intricate relationship with host organisms across various anatomical regions.

Currently, the understanding of the lung-gut axis is still undergoing continuous exploration. Unraveling the intricate interplay between the pulmonary and gastrointestinal systems could lead to a more comprehensive comprehension of the impact of commensal microbial communities as potential therapeutic targets for various respiratory diseases. The causal role of these gut microbiota in preventing asthma development is supported by studies demonstrating that infants at risk for asthma exhibit transient gut microbial dysbiosis within their first 100 days of life, and by microbiota transplantation experiments showing that specific commensal bacteria transplantation improves airway inflammation in adult offspring.<sup>46</sup> The interaction between lung and gut microbiota is complex. To better define the host-microbiota relationship, extensive experiments exploring specific bacterial functions have been conducted, such as fecal microbiota transplantation and breast milk microbial transplantation, which further investigate the protective effects provided by exogenous bacterial strains against lower respiratory tract infections.<sup>47,48</sup> The heatmap analysis in this study revealed a strong correlation between numerous bacterial flora in both lungs and guts, providing valuable references for future investigations into specific bacterial functions.

In conclusion, CpG-ODN administration can ameliorate OVA-induced asthma in mice by preserving the normal lung and intestinal structure, safeguarding the integrity of the mucosal mechanical barrier, and improving dysbiosis. Following treatment, beneficial bacteria and their metabolites exploit the microecology to modulate immune cells, participate in mucosal immune responses, and confer protective effects on the immune barrier. Moreover, the observed significant correlation between lung and gut microbiota provides valuable insights for future investigations into specific flora functions. *Treponemalspirillum* and *Clostridium* enrichment in response to CpG-ODN treatment could serve as biomarkers for exploring precise microbiota transplantation therapies for asthma. Notably, while *Clostridium* transplantation has demonstrated therapeutic efficacy against mouse models of asthma,<sup>49–51</sup> further research is warranted to elucidate *tremilspirillum*'s role through fecal microbiota transplantation experiments.

## Ethics Approval

Animal experiments have been reviewed and approved by the Animal Research Ethics Committee of Anhui Medical University (license number: LLSC20221231).

## Acknowledgments

This project is supported by the Anhui Provincial Higher Education Natural Science Foundation (KJ2021ZD0024).

## Author Contributions

All authors made a significant contribution to the work reported, whether that is in the conception, study design, execution, acquisition of data, analysis and interpretation, or in all these areas; took part in drafting, revising or critically reviewing the article; gave final approval of the version to be published; have agreed on the journal to which the article has been submitted; and agree to be accountable for all aspects of the work.

## Disclosure

All authors declare that they have no conflicts of interest in this work.

## References

1. Loftus PAAW, Sarah K. Epidemiology of asthma. *Curr Opin Otolaryngol Head Neck Surg*. 2016;24:245–249. doi:10.1097/moo.0000000000000262
2. Huang KAY, Ting X, Jianying Y, et al. Prevalence, risk factors, and management of asthma in China: a national cross-sectional study. *Lancet*. 2019;394:407–418. doi:10.1016/s0140-6736(19)31147-x

3. Stein MMAH, Gozdz CL, Igartua J, et al. Innate Immunity and Asthma Risk in Amish and Hutterite Farm Children. *N Engl J Med.* 2016;375:411–421. doi:10.1056/NEJMoa1508749
4. Roy S. Bacterial DNA in house and farm barn dust. *J Allergy Clin Immunol.* 2003;112:571–578. doi:10.1016/s0091-6749(03)01863-3
5. Krieg AMAY, Matson A-K, Waldschmidt S, et al. CpG motifs in bacterial DNA trigger direct B-cell activation. *Nature.* 1995;374:546–549. doi:10.1038/374546a0
6. KRIEG AMAM, Fisher, ERIC SARA. Oligodeoxynucleotide Modifications Determine the Magnitude of B Cell Stimulation by CpG Motifs. *Antisense Nucleic Acid Drug Dev.* 1996;6:133–139. doi:10.1089/oli.1.1996.6.133
7. Rakoff-Nahoum SAP, Eslami-Varzaneh J, Edberg F, et al. Recognition of Commensal Microflora by Toll-Like Receptors Is Required for Intestinal Homeostasis. *Cell.* 118:229–241.
8. Ballas ZKAK, Warren AM, Rasmussen T, et al. Divergent Therapeutic and Immunologic Effects of Oligodeoxynucleotides with Distinct CpG Motifs. *J Immunol.* 2001;167:4878–4886. doi:10.4049/jimmunol.167.9.4878
9. Li H-T, Tian-tuo Chen AZ, Zhuang-gui Y, et al. Intranasal administration of CpG oligodeoxynucleotides reduces lower airway inflammation in a murine model of combined allergic rhinitis and asthma syndrome. *Int Immunopharmacol.* 2015;28:390–398. doi:10.1016/j.intimp.2015.06.028
10. Fonseca DEAK, Joel N. Use of CpG oligonucleotides in treatment of asthma and allergic disease. *Adv. Drug Delivery Rev.* 2009;61:256–262. doi:10.1016/j.addr.2008.12.007
11. Kim D-HAS, Jung-Ho P, Lee H-JA, et al. CpG Oligodeoxynucleotide Inhibits Cockroach-Induced Asthma via Induction of IFN- $\gamma$ <sup>+</sup>Th1 Cells or Foxp3<sup>+</sup>Regulatory T Cells in the Lung. *Allergy Asthma Immunol Res.* 2016;8:264. doi:10.4168/aaair.2016.8.3.264
12. Campbell JD. A limited CpG-containing oligodeoxynucleotide therapy regimen induces sustained suppression of allergic airway inflammation in mice. *Thorax.* 2014;69:565–573. doi:10.1136/thoraxjnl-2013-204605
13. Okajima TAS, Namai S, Ogita F, et al. Free Feeding of CpG-Oligodeoxynucleotide Particles Prophylactically Attenuates Allergic Airway Inflammation and Hyperresponsiveness in Mice. *Front Immunol.* 2021;12. doi:10.3389/fimmu.2021.738041
14. Perrone EEAJ, Breed E, Dominguez E, et al. Mechanisms of Methicillin-Resistant Staphylococcus aureus Pneumonia–Induced Intestinal Epithelial Apoptosis. *Shock.* 2012;38:68–75. doi:10.1097/SHK.0b013e318259abdb
15. Wang JAL, Wei F, Lian H, et al. Respiratory influenza virus infection induces intestinal immune injury via microbiota-mediated Th17 cell–dependent inflammation. *J Exp Med.* 2014;211:2397–2410. doi:10.1084/jem.20140625
16. Gray JAO, Worthen K, Alenghat G, Whitsett T, Deshmukh Hitesh J. Intestinal commensal bacteria mediate lung mucosal immunity and promote resistance of newborn mice to infection. *Sci, trans med.* 2017;9. doi:10.1126/scitranslmed.aaf9412
17. Aggarwal NAK, Puah S, Ginette Ru Ying Kittelmann, Sandra Hwang, In Young Chang, Matthew Wook. Microbiome and Human Health: current Understanding, Engineering, and Enabling Technologies. *Chem. Rev.* 2022;123:31–72. doi:10.1021/acs.chemrev.2c00431
18. Li RAL, Zhou J. Lung microbiome: new insights into the pathogenesis of respiratory diseases. *Signal Transd Targ Therapy.* 2024;9. doi:10.1038/s41392-023-01722-y
19. Pickard JMAM, Kinnebrew CF, Abt MA, et al. Rapid fucosylation of intestinal epithelium sustains host–commensal symbiosis in sickness. *Nature.* 2014;514:638–641. doi:10.1038/nature13823
20. Pham Tu ANAC, Goulding S, Arasteh D, et al. Epithelial IL-22RA1-Mediated Fucosylation Promotes Intestinal Colonization Resistance to an Opportunistic Pathogen. *Cell Host Microbe.* 2014;16:504–516. doi:10.1016/j.chom.2014.08.017
21. Lei CAS, Rui X, Tan G, et al. Enteric VIP-producing neurons maintain gut microbiota homeostasis through regulating epithelium fucosylation. *Cell Host Microbe.* 2022;30:1417–1434.e1418. doi:10.1016/j.chom.2022.09.001
22. Wang YAY, Shigemori Y, Watanabe S, et al. Inhibitory/Suppressive Oligodeoxynucleotide Nanocapsules as Simple Oral Delivery Devices for Preventing Atopic Dermatitis in Mice. *Mol Ther.* 2015;23:297–309. doi:10.1038/mt.2014.239
23. Kayraklioglu NAS, Julia Gregory Alvord W, Klinman Dennis M. Effect of Calcium Carbonate Encapsulation on the Activity of Orally Administered CpG Oligonucleotides. *Mol Ther Nucleic Acids.* 2017;8:243–249. doi:10.1016/j.omtn.2017.06.015
24. Montamat GAL, Poli C, Klimek A, et al. CpG Adjuvant in Allergen-Specific Immunotherapy: finding the Sweet Spot for the Induction of Immune Tolerance. *Front Immunol.* 2021;12. doi:10.3389/fimmu.2021.590054
25. Chang Y-SAK, Kwon Y-K, Park H-S, et al. The Effect of CpG-Oligodeoxynucleotides with Different Backbone Structures and 3' Hexameric Deoxyriboguanosine Run Conjugation on the Treatment of Asthma in Mice. *J Korean Med Sci.* 2009;24:860. doi:10.3346/jkms.2009.24.5.860
26. Budden KFAG, Wood SL, Cooper DLA, et al. Emerging pathogenic links between microbiota and the gut–lung axis. *Nat Rev Microbiol.* 2016;15:55–63. doi:10.1038/nrmicro.2016.142
27. Benard AAD, Huglo P, Hoorelbeke D, Tonnel A, Wallaert A-B. Increased intestinal permeability in bronchial asthma. *J Allergy Clin Immunol.* 1996;97:1173–1178. doi:10.1016/s0091-6749(96)70181-1
28. Zhang KAO, Qiu X, Sun J, et al. Desulfovibrio desulfuricans aggravates atherosclerosis by enhancing intestinal permeability and endothelial TLR4/NF- $\kappa$ B pathway in Apoe mice. *Genes Dis.* 2023;10:239–253. doi:10.1016/j.gendis.2021.09.007
29. Marquis TJAW, Banach VJ, David B. Septic arthritis caused by Desulfovibrio desulfuricans: a case report and review of the literature. *Anaerobe.* 2021;70:102407. doi:10.1016/j.anaerobe.2021.102407
30. Verstreken IAL, Wauters W, Verhaegen G. Desulfovibrio desulfuricans Bacteremia in an Immunocompromised Host with a Liver Graft and Ulcerative Colitis. *J Clin Microbiol.* 2012;50:199–201. doi:10.1128/jcm.00987-11
31. Lee-Sarwar KAD, Momeni S, Kelly B, et al. Association of the gut microbiome and metabolome with wheeze frequency in childhood asthma. *J Allergy Clin Immunol.* 2022;150:325–336. doi:10.1016/j.jaci.2022.02.005
32. Garrett WSAG, Glimcher JJ, Laurie H. Homeostasis and Inflammation in the Intestine. *Cell.* 2010;140:859–870. doi:10.1016/j.cell.2010.01.023
33. Burger-van Paassen NAV, Audrey Puiman Patrycja J, van der S, et al. The regulation of intestinal mucin MUC2 expression by short-chain fatty acids: implications for epithelial protection. *Biochem. J.* 2009;420:211–219. doi:10.1042/bj20082222
34. Huang HAL, Jiang-Qi Y, Yong M. Regulation of TWIK-related potassium channel-1 (Trek1) restitutes intestinal epithelial barrier function. *Cell. Mol. Immunol.* 2015;13:110–118. doi:10.1038/cmi.2014.137
35. Tanoue TAA, Honda K. Development and maintenance of intestinal regulatory T cells. *Nat Rev Immunol.* 2016;16:295–309. doi:10.1038/nri.2016.36
36. Atarashi KAT, Shima T, Imaoka T, et al. Induction of Colonic Regulatory T Cells by Indigenous Clostridium Species. *Nature.* 2011;331:337–341. doi:10.1126/science.1198469

37. Atarashi KAT, Oshima T, Suda K, et al. Treg induction by a rationally selected mixture of Clostridia strains from the human microbiota. *Nature*. 2013;500:232–236. doi:10.1038/nature12331
38. Herbst TAS, Schär A, Yadava C, et al. Dysregulation of Allergic Airway Inflammation in the Absence of Microbial Colonization. *Am J Respir Crit Care Med*. 2011;184:198–205. doi:10.1164/rccm.201010-1574OC
39. Barcik WAB, Rozlyn CTS, Milena Brett Finlay B. The Role of Lung and Gut Microbiota in the Pathology of Asthma. *Immunity*. 2020;52:241–255. doi:10.1016/j.immuni.2020.01.007
40. Bernard HAD, Bartke J-L, Kleinjans N, et al. Dietary Pectin–Derived Acidic Oligosaccharides Improve the Pulmonary Bacterial Clearance of *Pseudomonas aeruginosa* Lung Infection in Mice by Modulating Intestinal Microbiota and Immunity. *J Infect Dis*. 2014;211:156–165. doi:10.1093/infdis/jiu391
41. Kawahara TAT, Oishi T, Tanaka K, et al. Consecutive oral administration of *Bifidobacterium longum* MM-2 improves the defense system against influenza virus infection by enhancing natural killer cell activity in a murine model. *Microbiol Immunol*. 2015;59:1–12. doi:10.1111/1348-0421.12210
42. H WNPA, Pyne PL, David B, et al. Probiotic supplementation for respiratory and gastrointestinal illness symptoms in healthy physically active individuals. *Clin Nutr*. 2014;33:581–587. doi:10.1016/j.clnu.2013.10.002
43. Wang WAL, Zhang X, Qin H. *Bifidobacterium infantis* Relieves Allergic Asthma in Mice by Regulating Th1/Th2. *Med Sci Monit*. 2020;26. doi:10.12659/msm.920583
44. Ghorbani PAS, Prisila H, Djiadeu Q, et al. Short-chain fatty acids affect cystic fibrosis airway inflammation and bacterial growth. *Eur Respir J*. 2015;46:1033–1045. doi:10.1183/09031936.00143614
45. G TAA, Yadava ES, Sichelstiel K, et al. Gut microbiota metabolism of dietary fiber influences allergic airway disease and hematopoiesis. *Nature Med*. 2014;20:159–166. doi:10.1038/nm.3444
46. S AMCA, Leah T, Dimitriu Pedro A, et al. Early infancy microbial and metabolic alterations affect risk of childhood asthma. *Sci, trans med*. 2015;7. doi:10.1126/scitranslmed.aab2271
47. Petrof EOAG, Vanner GB, Weese SJ, et al. Stool substitute transplant therapy for the eradication of *Clostridium difficile* infection: ‘RePOOPulating’ the gut. *Microbiome*. 2013;1. doi:10.1186/2049-2618-1-3
48. Amin Sikder M A R A, Ridwan B, Tufael Sebina A, et al. Maternal diet modulates the infant microbiome and intestinal Flt3L necessary for dendritic cell development and immunity to respiratory infection. *Immunity*. 2023;56:1098–1114.e1010. doi:10.1016/j.immuni.2023.03.002
49. Z HFA, Bai Y, Wang X-Q, et al. *Clostridium leptum* induces the generation of interleukin-10+ regulatory B cells to alleviate airway inflammation in asthma. *Mol Immunol*. 2022;145:124–138. doi:10.1016/j.molimm.2022.03.010
50. Huang FAQ, Yin H-M, Jia-ning Gao, et al Early-Life Exposure to *Clostridium leptum* Causes Pulmonary Immunosuppression. *PLoS One*. 2015;10: e0141717. doi:10.1371/journal.pone.0141717
51. Li Y-NAH, Liu F, Qiao L, et al. Effect of oral feeding with *Clostridium leptum* on regulatory T-cell responses and allergic airway inflammation in mice. *Ann Allergy Asthma Immunol*. 2012;109:201–207. doi:10.1016/j.anai.2012.06.017

## Journal of Inflammation Research

### Publish your work in this journal

The Journal of Inflammation Research is an international, peer-reviewed open-access journal that welcomes laboratory and clinical findings on the molecular basis, cell biology and pharmacology of inflammation including original research, reviews, symposium reports, hypothesis formation and commentaries on: acute/chronic inflammation; mediators of inflammation; cellular processes; molecular mechanisms; pharmacology and novel anti-inflammatory drugs; clinical conditions involving inflammation. The manuscript management system is completely online and includes a very quick and fair peer-review system. Visit <http://www.dovepress.com/testimonials.php> to read real quotes from published authors.

Submit your manuscript here: <https://www.dovepress.com/journal-of-inflammation-research-journal>

**Dovepress**  
Taylor & Francis Group